Buffer Interference with Protein Dynamics: A Case Study on Human Liver Fatty Acid Binding Protein

Dong Long and Daiwen Yang*
Department of Biological Sciences, National University of Singapore, Singapore 117543

ABSTRACT Selection of suitable buffer types is often a crucial step for generating appropriate protein samples for NMR and x-ray crystallographic studies. Although the possible interaction between MES buffer (2-(*N*-morpholino)ethanesulfonic acid) and proteins has been discussed previously, the interaction is usually thought to have no significant effects on the structures of proteins. In this study, we demonstrate the direct, albeit weak, interaction between MES and human liver fatty acid binding protein (hLFABP). Rather than affecting the structure of hLFABP, we found that the dynamics of hLFABP, which were previously proposed to be relevant to its functions, were significantly affected by the binding of hLFABP with MES. Buffer interference with protein dynamics was also demonstrated with Bis-Tris buffer, which is quite different from MES and fatty acids in terms of their molecular structures and properties. This result, to our knowledge, is the first published report on buffer interference with protein dynamics on a microsecond to millisecond timescale and could represent a generic problem in the studies of functionally relevant protein dynamics. Although being a fortuity, our finding of buffer-induced changes in protein dynamics offers a clue to how hLFABP accommodates its ligands.

INTRODUCTION

The development of NMR hardware and methodology during the past several decades has made the determination of protein structure at atomic resolution and the characterization of protein dynamics on various timescales routine work in many NMR laboratories. In addition, structural genomics has further facilitated high-throughput determination of protein structures. However, a fundamental problem—often a bottleneck—in most structural biology projects is the difficulty of preparing protein samples that are suitable for NMR experiments. Types of buffers have long been thought to play an important role in maintaining protein solubility and stability (1). Although some general guidelines have been proposed for buffer selection (2), screening a large number of buffer types is still crucial in most cases to identify suitable buffers. Compounds that destabilize protein structures are usually thought to bind proteins directly and interact favorably with the unfolded state, whereas compounds that are excluded from the protein surface are thought to leave proteins hydrated (1).

Some structural biology studies have demonstrated that protein samples prepared in certain buffers might form complexes with buffer agents (3–8). However, because it is generally believed that such interactions have no significant influence on protein structures, the effects that some buffers have on protein samples have been largely ignored in practice. Yet, because of growing evidence showing that protein dynamics, in addition to three-dimensional structures, are highly relevant to biological functions (9,10), the effects of buffers on protein dynamics deserve the attention of protein scientists. The influence on protein dynamics by the buffer-protein interaction has been discussed in the literature (e.g., the studies by Zhang et al. (3), Ganichkin et al. (8), and Pascal et al. (11)). For example, crystallographic studies on selenocysteine synthase suggested that the binding of phosphate to the protein would trigger a disorder-order transition of a loop region (8). Pascal et al. (8) also noticed the effect of phosphate buffer on the Src homology 2 domain due to the direct binding of phosphate ions to the protein (11). However, to our knowledge, scientists are not yet aware of the magnitude of changes in protein dynamics caused by protein-buffer agent interactions, especially on the microsecond to millisecond timescale.

In this study, we investigated the potential interaction between buffer agents and human liver fatty acid binding protein (hLFABP). hLFABP is highly flexible on millisecond timescales (12), and this property of slow dynamics has been previously proposed as being relevant to how this protein accommodates its ligands inside the protein cavity. MES buffer (2-(*N*-morpholino)ethanesulfonic acid) is one of Good's buffers; it is widely used in various biological studies and believed to have no or low interference with protein analysis (13,14). Nevertheless, the influences of MES, as well as other buffer agents, on protein dynamics on the picosecond to nanosecond timescale and on the microsecond to millisecond timescale are rarely investigated. Because MES buffer can maintain a stable pH environment at 5.5, which deviates significantly from the theoretical isoelectric point of hLFABP (~6.60, as estimated with ProtParam, ExPASy), this buffer seems to be a good choice to use with hLFABP. In this work, we report the direct interaction between MES and hLFABP in aqueous solution and demonstrate the interference of MES with hLFABP dynamics on a millisecond timescale. To test whether the

Submitted May 25, 2008, and accepted for publication October 9, 2008.

*Correspondence: dbsydw@nus.edu.sg

Editor: Arthur G. Palmer 3rd.

0006-3495/09/02/1482/7 $2.00

doi: 10.1016/j.bpj.2008.10.049

observed buffer effect was an incidental case, we also measured the change of the protein's slow motions in Bis-Tris buffer, which possesses very dissimilar properties and a different chemical structure than MES and than fatty acids (the natural ligands of hLFABP). The result shows that the buffer's interference with protein dynamics could be a relatively generic phenomenon that should not be ignored.

MATERIALS AND METHODS

Protein purification and NMR sample preparation

The cDNA coding hLFABP was subcloned into a pET32a-derived overexpression vector and was expressed in *Escherichia coli* BL21(DE3). M9 minimum medium containing ^{15}N-labeled NH_4Cl as the sole nitrogen source was used for isotope labeling of this protein. hLFABP expression was induced by adding isopropyl-beta-D-1-thiogalactopyranoside (IPTG) to a final concentration of 1 mM. After the cultures were further incubated at 20°C overnight, *E. coli* cells were harvested and then lysed by sonication. The purification of His-tagged hLFABP was carried out with Ni-NTA affinity chromatography under native conditions (15), after which fast protein size-exclusion liquid chromatography was performed. Delipidation of purified hLFABP followed the previously established protocol at 37°C (16). By thorough buffer exchange, ^{15}N-labeled hLFABP samples were prepared in three solutions: solution I (50 mM NaCl, 1 mM EDTA, pH 5.5), solution II (50 mM MES, 50 mM NaCl, 1 mM EDTA, pH 5.5), and solution III (50 mM Bis-Tris, 50 mM NaCl, 1 mM EDTA, pH 5.8), respectively.

MES titration of hLFABP

^{15}N-labeled hLFABP with a concentration of ~0.4 mM was prepared in solution I for the titration experiment at 35°C. Concentrated MES solution (100 and 500 mM MES with the presence of 50 mM NaCl, pH 5.5) was titrated into protein solution. Heteronuclear single quantum correlation (HSQC) spectra at respective MES concentrations of 9, 19, 31, and 51 mM were recorded on an 800 MHz spectrometer (Avance; Bruker Biospin) equipped with a cryoprobe at 35°C. Combined chemical shift perturbations (CCSP) were calculated using Eq. 1 as follows:

$$\Delta_{\mathrm{ppm}} = \left[(\Delta\delta_{\mathrm{HN}})^2 + (\Delta\delta_{\mathrm{N}} * \alpha_{\mathrm{N}})^2\right]^{1/2} \quad (1)$$

where $\Delta\delta_{HN}$ and $\Delta\delta_N$ are the respective differences of ^1H and ^{15}N chemical shifts in the absence of MES and 51 mM MES; α_N is a scaling factor with a value of 0.17 (17).

NMR spectroscopy

^{15}N relaxation times T_1 and $T_{1\rho}$, and ^1H-^{15}N nuclear Overhauser effects (NOEs) were measured on a 500 MHz spectrometer (Avance; Bruker Biospin) equipped with a cryoprobe using inverse-detected two-dimensional NMR methods at 35°C for hLFABP (~1 mM) in both solutions I and II (18,19). Six points with relaxation delays of 5, 60, 150, 250, 360, and 505 ms were collected for the determination of T_1 values. $T_{1\rho}$ values were determined by collecting seven points with delays of 5, 20, 40, 60, 80, 100, and 125 ms using a spin-lock field strength of 1600 Hz. Two spectra with and without proton saturation were recorded for the measurement of heteronuclear NOEs. Proton saturation time was 2.5 s, whereas the recycle delay also was 2.5 s. The calculation of T_2 values from T_1 and $T_{1\rho}$ were carried out as described previously (19). Values of order parameter (S^2), localized rotational correlation time (τ_{loc}), and effective correlation time (τ_e) were extracted on a per residue basis from T_1, T_2, and NOE data using a simple method based on the Lipari-Szabo model, as described previously (20). This method can be used to obtain dynamics parameters for nonspherical proteins including unfolded proteins. Relaxation dispersion spectra (12,21) were recorded at 500 MHz and 800 MHz for hLFABP in solution I and solution II at 35°C. A constant delay of 50 ms was used with a series of Carr-Purcell-Meiboom-Gill (CPMG) field strengths (40, 80, 120, 160, 200, 240, 280, 320, 400, 480, 560, 640, 800, and 960 Hz). Dispersion curves were subsequently fitted with a two-site exchange model to extract kinetics parameters. Relaxation dispersion spectra for hLFABP in solution III were also recorded at a field strength of 800 MHz.

RESULTS AND DISCUSSION

MES binding inducing chemical shift perturbation

Chemical shifts are highly sensitive to changes of local magnetic environment, and thus can be used as powerful probes to pinpoint residues involved in protein-ligand contacts. A number of residues in hLFABP displayed gradual chemical shift changes (Fig. 1) as MES concentrations increased from 0 to ~50 mM (the normal buffering concentration used in biochemical studies). The result shows that MES-hLFABP interactions are somewhat weak because the binding was not saturated even when the ligand (MES) concentration was >100× larger than the protein. The chemical exchange between MES-free and MES-bound hLFABP forms is a fast process in the chemical shift time regime because only one single resonance signal was observed for each amide in each titration HSQC spectrum. On the basis of CCSP (with a cutoff of 0.05 ppm) shown in Fig. 2 and the backbone resonance assignment of hLFABP (22), the residues involved in the interactions were identified as both polar (Q10, T53, T55, E74, T75, T95, N99, N113, K123, and R124) and nonpolar (G39, I54, I61, V94, V103, and M115) residues (Figs. 2 and 3). On the basis of chemical shift perturbation alone, we could not determine the exact binding sites because allosteric effects can result in chemical shift changes of some residues distant from the binding sites. Nevertheless, the results indicate that the binding could be mediated by different types of interactions – hydrogen bonds and hydrophobic interactions—a hypothesis that agrees well with the previous crystallographic study on the metallo-beta-lactamase/MES complex (4). Furthermore, MES, which is a zwitterion, could form electrostatic interactions with both positively charged residues (e.g., K123 and R124) and negatively charged residues (e.g., E74). Although MES interacts directly with hLFABP, the overall tertiary protein structure should be the same in the presence and absence of MES. This observation is supported by the finding that only a small number of residues displayed relatively small chemical shift changes (<0.2 ppm) upon the binding of MES to hLFABP.

Effects of MES binding on protein dynamics on the picosecond to nanosecond timescale

^{15}N relaxation measurements are commonly used to probe protein backbone dynamics (23). For rat intestinal fatty acid binding protein (IFABP), there is debate over whether the role of fast motions along the backbone on picosecond to nanosecond timescales is related to the function of IFABP in cellular fatty acid transport and targeting (24,25). Thus, it is

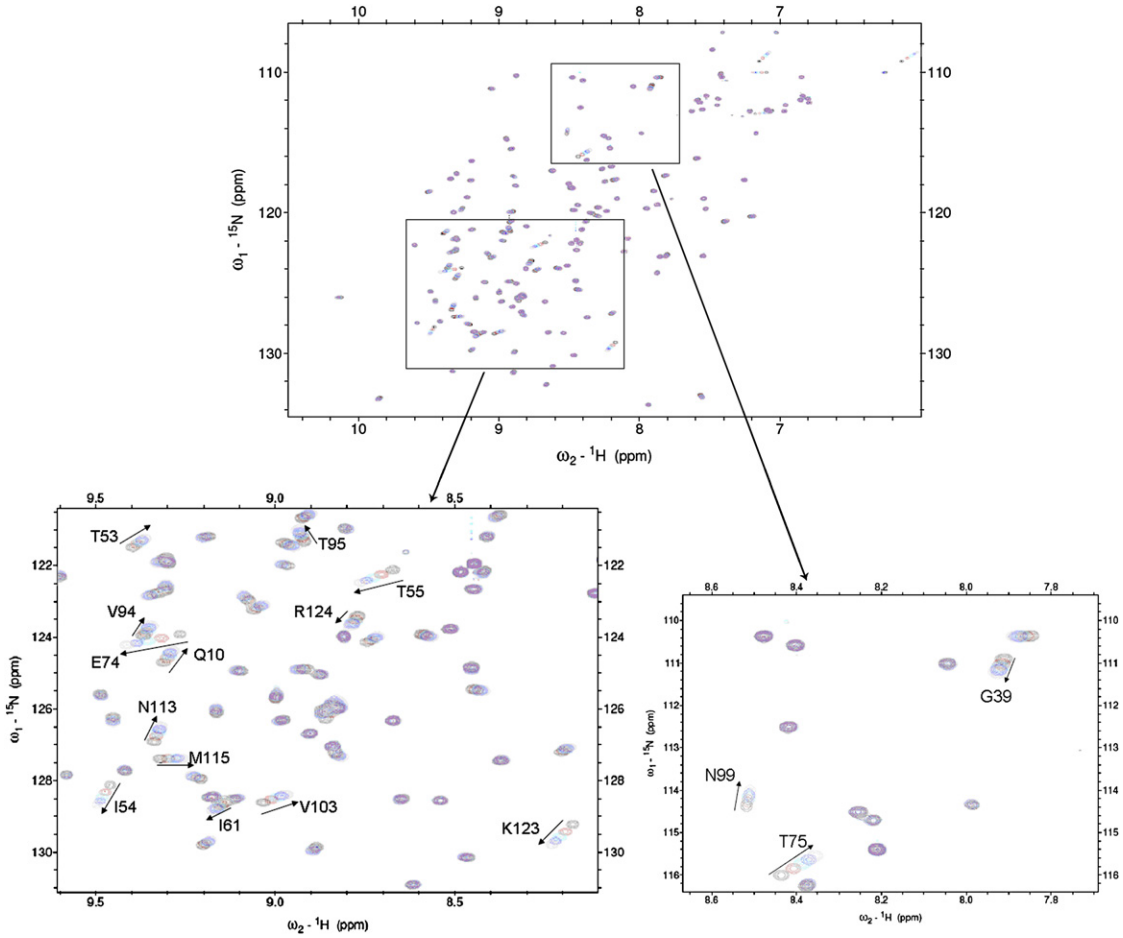

FIGURE 1 Overlay of ^{15}N-^{1}H HSQC spectra of ~0.4 mM protein with 50 mM NaCl, pH 5.5, and a series of MES concentrations: 0 mM (*black*), 9 mM (*red*), 19 mM (*cyan*), 31 mM (*blue*), and 51 mM (*pink*). The direction of the change of peak positions from 0 MES to 51 mM MES is indicated by an arrow.

interesting to know whether MES, which also binds LFABP (although with a much weaker affinity), can induce any changes in fast motions in protein dynamics. Model-free analysis for both MES-bound and MES-free proteins was performed to extract dynamical parameters for individual residues (19,20). Calculated values of generalized order parameters (S^2) are shown in Fig. 4 *A*, and the patterns for these two forms are very similar to each other. Although the S^2 values of a majority of residues increased in the presence of MES, the changes in S^2 were very small (~0.02 on average). In contrast to S^2, the τ_{loc} values for all residues increased significantly in the presence of MES (Fig. 4 *B*), and the average change was 0.84 ns. This finding could probably be caused by the enlarged, hydrated size of the hLFABP/MES complex and/or transient protein aggregation formed in the presence of MES. The slight increase in S^2 may also result from transient aggregation (26).

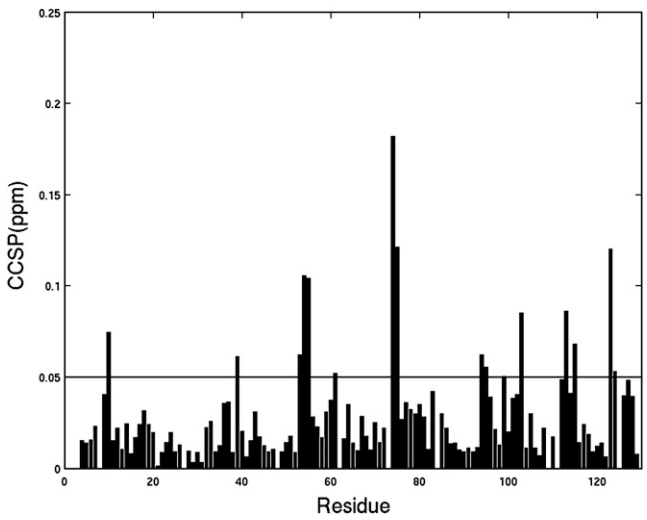

FIGURE 2 Histogram of CCSP of hLFABP upon titration with MES. The ^{1}H and ^{15}N chemical shifts are normalized using a scaling factor of 0.17.

Effects of MES binding on protein dynamics on the microsecond to millisecond timescale

We recently modified the conventional relaxation-compensated CPMG experiment (21,27) by incorporating a four-step phase-cycling scheme developed by Yip and Zuiderweg (28), which greatly suppresses the resonance offset and pulse imperfection effects. With the combination of the four-step phase-cycling scheme and the conventional CPMG element,

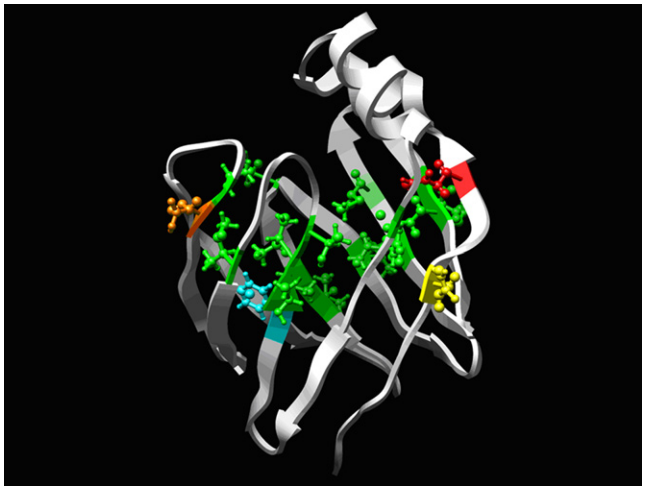

FIGURE 3 Residues that are significantly perturbed by MES (as labeled in Fig. 1) are shown as green, yellow, or brown. Q10 and E74 are shown as yellow and brown, respectively. Q14 and F52 are red and cyan, respectively. Protein structure is displayed using UCSF Chimera.

the modified CPMG experiment is nearly free from systematic errors; it also provides the same number of accessible CPMG field strengths (ν_{CP}) as the conventional CPMG when a constant-time CPMG scheme is used (12). Using this modified experiment (12), we measured the relaxation dispersion profiles of hLFABP in the presence and absence of MES. Due to the difference of the apparent rotational diffusion coefficients of hLFABP in the presence and absence of MES, effective transverse relaxation rates (R_2^{eff}) for all residues were significantly greater in the presence of MES than in the absence of MES (Fig. 5). To visualize the influence of MES on the dispersion profiles (or slow dynamics), the apparent diffusion effect was corrected; the corrected profiles are also shown in Fig. 5. Slow dynamics of residues directly involved in binding (as shown by titration studies) could be influenced by MES (e.g., Q10), but this occurrence is not a general rule. For example, residue E74, which forms direct contact with MES, did not display any change in slow motions, which was within the experimental error (Fig. 5). Quite unexpectedly, some residues that did not display any chemical shift perturbations upon MES titration showed significant changes in slow dynamics. Two such examples (Q14 and F52) are shown in Fig. 5. The fast chemical exchange between the MES-free and MES-bound hLFABP forms could contribute to the exchange-induced transverse relaxation (R_{ex}), but the contribution should be proportional to the ^{15}N chemical shift differences between the two forms. Instead, the changes in the relaxation dispersion profiles did not correlate with the chemical shift differences. In principle, transient aggregation, which could be one of the reasons for the increase of the rotational correlation time, might also contribute to $R_{ex.}$ Such an effect, however, should be global and introduce R_{ex} to all residues at the aggregation interface, including those residues even without conformational dynamics in solution I. However, almost all the residues that did not show conformational dynamics in solution I were not found to have R_{ex} in solution II. Furthermore, some residues (e.g., E74) directly involved in binding did not demonstrate any change in R_{ex} either. Therefore, we believe the change in slow dynamics must be caused by the alternation of intrinsic protein dynamics.

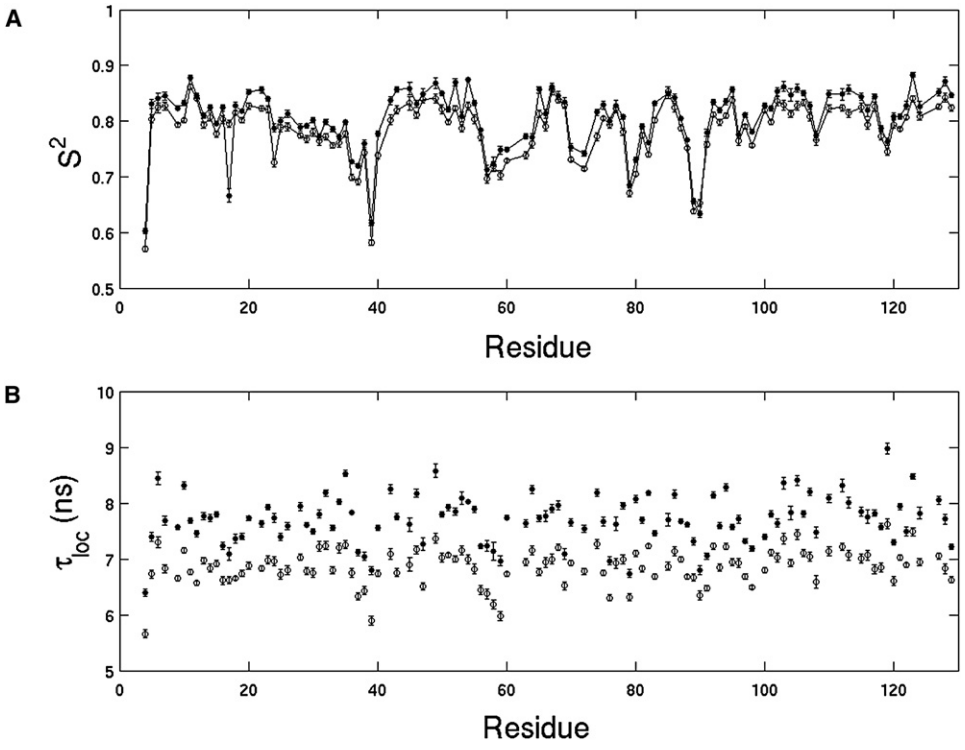

FIGURE 4 (*A*) Comparison of generalized order parameters for MES-bound (*solid circles*) and MES-free (*open circles*) hLFABP. (*B*) Comparison of localized rotational correlation times for MES-bound (*solid circles*) and MES-free (*open circles*) hLFABP.

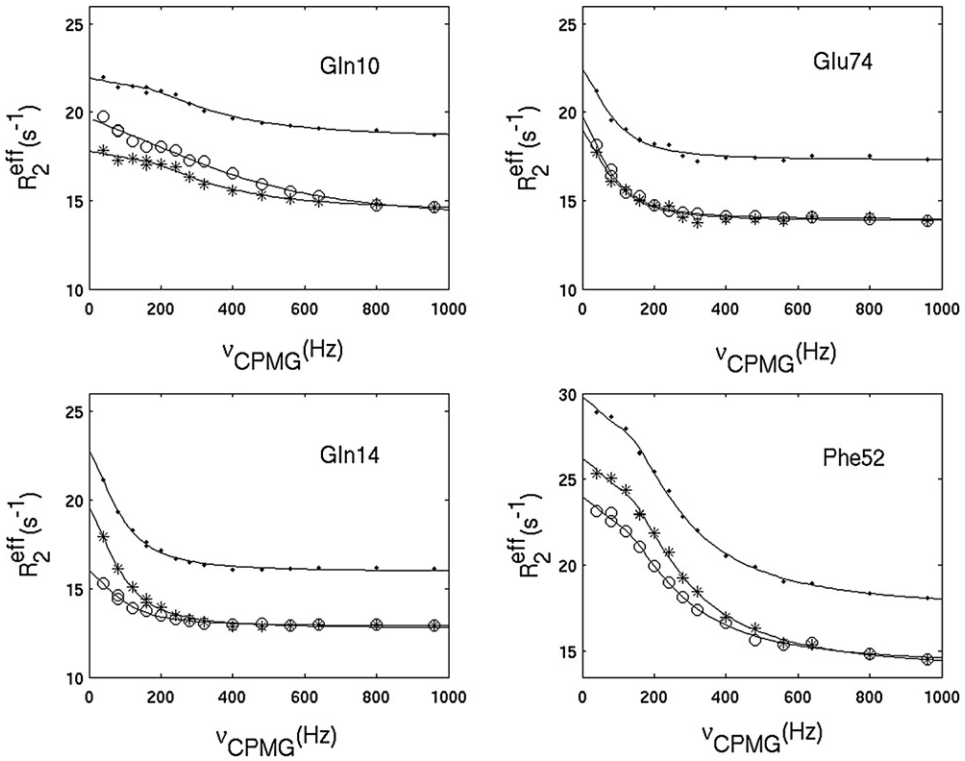

FIGURE 5 Relaxation dispersion curves measured in the absence (*open circles*) and presence (*solid circles*) of MES at an 800 MHz ^{1}H frequency. Solid lines are fitting curves of experimental data to a two-site exchange model. For the purpose of comparative illustration, each dispersion curve measured in the presence (*solid circles*) of MES is shifted down by a value of the difference between $R_2^{eff}(\nu_{CP} = 960$ Hz) values in the absence and presence of MES. The shifted curves are represented by asterisks.

Kinetics parameters extracted from a two-site exchange model showed that MES binding increased the exchange rates (k_{ex}) for Q14 and F52 by 105% and 55%, respectively, leaving the population of each state and chemical shift difference ($\Delta\omega$) between the two states almost unchanged. Although Q14 and F52 do not interact directly with MES based on chemical shift perturbation results, they are spatially close by the residues that can directly interact with MES. It is clear that the kinetics parameters obtained in the presence and absence of MES can be significantly different. Therefore, protein dynamics probed by NMR could be complicated by the use of buffer types.

Commonality of buffer interference with protein dynamics

Binding of MES to hLFABP seems to be nonanalogous to the hLFABP-fatty acid interaction because the residues involved in binding with MES, shown by the chemical shift perturbation, are different from the binding sites of fatty acids, which are the natural ligands of FABPs (29). Thus, we surmise that the buffer effect on protein dynamics could be a generic problem in the studies of protein dynamics and that MES is not the sole example. To validate this conjecture, we examined the potential interaction between hLFABP and Bis-Tris buffer and the change of protein slow dynamics due to this interaction. Bis-Tris, as a cation buffer with a very different chemical structure from fatty acids, should not have any preferable interaction with hLFABP analogous to fatty acids.

In fact, chemical shift perturbation was also observed in Bis-Tris buffer, although the perturbation in the number of residues and the magnitude of chemical shifts were both smaller than those in MES (Fig. 6). This result demonstrated that there was still a weak interaction between the Bis-Tris buffer agent and hLFABP. Also, as in the experiment with MES buffer, slow dynamics of the residues at or close to the potential binding sites was significantly perturbed by the binding of Bis-Tris (Fig. 7).

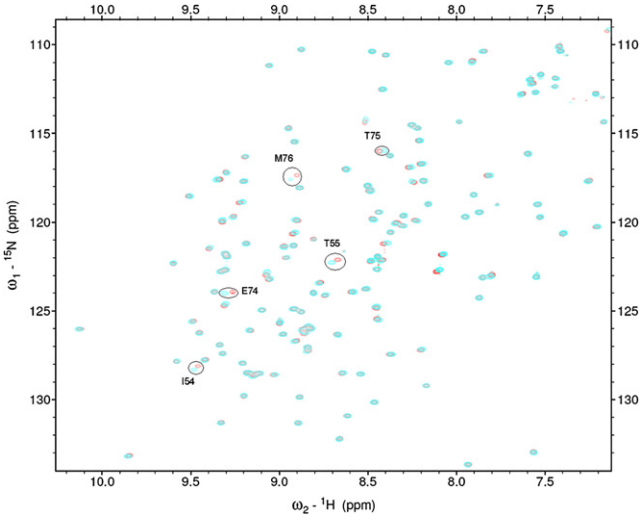

FIGURE 6 Overlay of ^{15}N-^{1}H HSQC spectra of ~0.4 mM hLFABP in solution I (*red*) and solution III (*cyan*). Residues, which showed significant resonance shift, are circled.

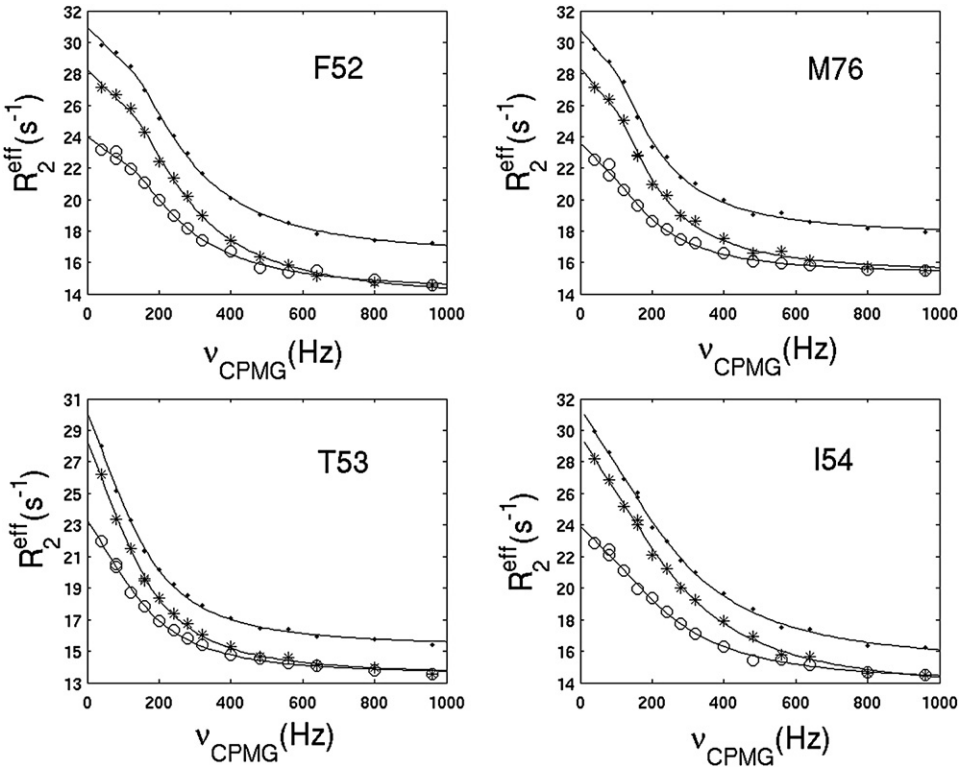

FIGURE 7 Relaxation dispersion curves of hLFABP measured in solution I (*open circles*) and solution III (*solid circles*) at an 800 MHz ^{1}H frequency. Solid lines are fitting curves of experimental data to a two-site exchange model. For the purpose of comparative illustration, each dispersion curve measured in solution III (*solid circles*) is shifted down by a value of the difference between $R_2^{eff}(\nu_{CP} = 960$ Hz) values in solution I and III. The shifted curves are represented by asterisks.

Our results showed that inappropriate buffer selection would seriously influence and complicate the analysis of the functional dynamics of hLFABP. And this could be a general phenomenon occurring in other dynamical systems. Because buffer screening is routinely conducted in structural biology laboratories, our results should warrant the special attention of scientists when they study the relationship between the function and dynamics of proteins.

Further implications

The structures of proteins belonging to the FABP family have been known for almost two decades. However, high-resolution three-dimensional structures have not demonstrated how FABPs accommodate ligands; this is because crystal structures (30) do not show any obvious opening on the protein surface that would allow ligands to penetrate and reach the ligand binding site inside the cavity of the β-barrel. Thus, many efforts have been made in the past decade to explore the dynamics of FABPs (24,31,32). Recent work using molecular dynamics simulations on the interaction between FABPs and fatty acids (31,32) has demonstrated that the adsorption of the ligand on the protein surface at the vicinity of the portal region is an important process that occurs at the early stage of the ligand-protein interaction. However, the biophysical significance of this adsorption is not yet fully understood. Here, our results suggest that this initial adsorption process has an important role. Because we have demonstrated that the binding of proteins with MES and Bis-Tris buffers induces significant changes of the conformational dynamics of the residues in and close to the binding regions, the initial adsorption of fatty acid on the protein surface in close proximity to the portal region could possibly also induce change in the conformational dynamics of the portal area, thus allowing ligand entry through a significantly reorganized conformation.

This work was supported by grant R154000272305 from the Biomedical Research Council (BMRC) and the Agency for Science, Technology and Research (A*STAR)of Singapore. D. L. is a recipient of the National University of Singapore (NUS) Research Scholarship.

REFERENCES

1. Bagby, S., K. I. Tong, and M. Ikura. 2001. Optimization of protein solubility and stability for protein nuclear magnetic resonance. *Methods Enzymol.* 339:20–40.
2. Kremer, W., and H. R. Kalbitzer. 2001. Physiological conditions and practicality for protein nuclear magnetic resonance spectroscopy: experimental methodologies and theoretical background. *Methods Enzymol.* 339:3–19.
3. Zhang, M., M. Zhou, R. L. Van Etten, and C. V. Stauffacher. 1997. Crystal structure of bovine low molecular weight phosphotyrosyl phosphatase complexed with the transition state analog vanadate. *Biochemistry.* 36:15–23.
4. Fitzgerald, P. M. D., J. K. Wu, and J. H. Toney. 1998. Unanticipated inhibition of the metallo-beta-lactamase from Bacteroides fragilis by 4-morpholineethanesulfonic acid (MES): a crystallographic study at 1.85-Å resolution. *Biochemistry.* 37:6791–6800.
5. Shirai, T., Y. Matsui, C. Shionyu-Mitsuyama, T. Yamane, H. Kamiya, et al. 2002. Crystal structure of a conger eel galectin (congerin II) at 1.45 Å resolution: implication for the accelerated evolution of a new

ligand-binding site following gene duplication. *J. Mol. Biol.* 321:879–889.

6. Oakley, A. J., M. L. Bello, G. Ricci, G. Federici, and M. W. Parker. 1998. Evidence for an induced-fit mechanism operating in pi class glutathione transferases. *Biochemistry.* 37:9912–9917.
7. Whittington, D. A., M. L. Wise, M. Urbansky, R. M. Coates, R. B. Croteau, et al. 2002. Bornyl diphosphate synthase: structure and strategy for carbocation manipulation by a terpenoid cyclase. *Proc. Natl. Acad. Sci. USA.* 99:15375–15380.
8. Ganichkin, O. M., X. M. Xu, B. A. Carlson, H. Mix, D. L. Hatfield, et al. 2008. Structure and catalytic mechanism of eukaryotic selenocysteine synthase. *J. Biol. Chem.* 283:5849–5865.
9. Eisenmesser, E. Z., D. A. Bosco, M. Akke, and D. Kern. 2002. Enzyme dynamics during catalysis. *Science.* 295:1520–1523.
10. Mittermaier, A., and L. E. Kay. 2006. New tools provide new insights in NMR studies of protein dynamics. *Science.* 312:224–228.
11. Pascal, S. M., T. Yamazaki, A. U. Singer, L. E. Kay, and J. D. Forman-Kay. 1995. Structural and dynamic characterization of the phosphotyrosine binding region of a Src homology 2 domain–phosphopeptide complex by NMR relaxation, proton exchange, and chemical shift approaches. *Biochemistry.* 34:11353–11362.
12. Long, D., M. Liu, and D. Yang. 2008. Accurately probing slow motions on millisecond timescales with a robust NMR relaxation experiment. *J. Am. Chem. Soc.* 130:2432–2433.
13. Good, N. E., G. D. Winger, W. Winter, T. N. Connolly, S. Izawa, et al. 1966. Hydrogen ion buffers for biological research. *Biochemistry.* 5:467–477.
14. Yu, Q., A. Kandegedara, Y. Xu, and D. B. Rorabacher. 1997. Avoiding interferences from Good's buffers: a contiguous series of noncomplexing tertiary amine buffers covering the entire range of pH 3–11. *Anal. Biochem.* 253:50–56.
15. Qiagen 2003. The QIAexpressionist: A Handbook for High-Level Expression and Purification of 6xHis-Tagged Proteins. Qiagen, Valencia, CA.
16. Glatz, J. F., and J. H. Veerkamp. 1983. Removal of fatty acids from serum albumin by Lipidex 1000 chromatography. *J. Biochem. Biophys. Methods.* 8:57–61.
17. Piserchio, A., M. Pellegrini, S. Mehta, S. M. Blackman, E. P. Garcia, et al. 2002. The PDZ1 domain of SAP90: characterization of structure and binding. *J. Biol. Chem.* 277:6967–6973.
18. Farrow, N. A., O. Zhang, J. D. Forman-Kay, and L. E. Kay. 1995. Comparison of the backbone dynamics of a folded and an unfolded SH3 domain existing in equilibrium in aqueous buffer. *Biochemistry.* 34:868–878.
19. Ran, X., H. H. Miao, F. S. Sheu, and D. Yang. 2003. Structural and dynamic characterization of a neuron-specific protein kinase C substrate, neurogranin. *Biochemistry.* 42:5143–5150.
20. Yang, D., Y. K. Mok, J. D. Forman-Kay, N. A. Farrow, and L. E. Kay. 1997. Contributions to protein entropy and heat capacity from bond vector motions measured by NMR spin relaxation. *J. Mol. Biol.* 272:790–804.
21. Tollinger, M., N. R. Skrynnikov, F. A. Mulder, J. D. Forman-Kay, and L. E. Kay. 2001. Slow dynamics in folded and unfolded states of an SH3 domain. *J. Am. Chem. Soc.* 123:11341–11352.
22. Xu, Y., D. Long, and D. Yang. 2007. Rapid data collection for protein structure determination by NMR spectroscopy. *J. Am. Chem. Soc.* 129:7722–7723.
23. Kay, L. E. 1998. Protein dynamics from NMR. *Nat. Struct. Biol.* 5:513–517.
24. Hodsdon, M. E., and D. P. Cistola. 1997. Ligand binding alters the backbone mobility of intestinal fatty acid-binding protein as monitored by 15N NMR relaxation and 1H exchange. *Biochemistry.* 36:2278–2290.
25. Zhang, X., X. Sui, and D. Yang. 2006. Probing methyl dynamics from 13C auto- and cross-correlated relaxation. *J. Am. Chem. Soc.* 128:5073–5081.
26. Schurr, J. M., H. P. Babcock, and B. S. Fujimoto. 1994. A test of the model-free formulas. Effects of anisotropic rotational diffusion and dimerization. *J. Magn. Reson. B.* 105:211–224.
27. Loria, J. P., M. Rance, and A. G. Palmer. 1999. A relaxation-compensated Carr-Purcell-Meiboom-Gill sequence for characterizing chemical exchange by NMR spectroscopy. *J. Am. Chem. Soc.* 121:2331–2332.
28. Yip, G. N., and E. R. Zuiderweg. 2004. A phase cycle scheme that significantly suppresses offset-dependent artifacts in the R2-CPMG 15N relaxation experiment. *J. Magn. Reson.* 171:25–36.
29. He, Y., X. Yang, H. Wang, R. Estephan, F. Francis, et al. 2007. Solution-state molecular structure of apo and oleate-liganded liver fatty acid-binding protein. *Biochemistry.* 46:12543–12556.
30. Sacchettini, J. C., J. I. Gordon, and L. J. Banazak. 1989. Crystal structure of rat intestinal fatty-acid-binding protein: refinement and analysis of the Escherichia coli-derived protein with bound palmitate. *J. Mol. Biol.* 208:327–339.
31. Friedman, R., E. Nachliel, and M. Gutman. 2006. Fatty acid binding proteins: same structure but different binding mechanisms? Molecular dynamics simulations of intestinal fatty acid binding protein. *Biophys. J.* 90:1535–1545.
32. Tsfadia, Y., R. Friedman, J. Kadmon, A. Selzer, E. Nachliel, et al. 2007. Molecular dynamics simulations of palmitate entry into the hydrophobic pocket of the fatty acid binding protein. *FEBS Lett.* 581:1243–1247.